Continuum mechanics and thermodynamics manuscript No.
(will be inserted by the editor)

Thermodynamic framework for variance-based non-local constitutive models

Charles Mareau

Received: date / Accepted: date

Abstract The present work deals with the development of a framework dedicated to the construction of constitutive models with non-local internal variables. Such internal variables allow considering the impact of microstructural changes on the current state of a material point. Non-locality is introduced by considering, not only the spatial average, but also the spatial variance of an internal variable in constitutive relations. The proposed framework relies on continuum thermodynamics to construct the set of constitutive equations. Such a framework allows including some information regarding the spatial distribution of internal variables when constructing non-local models for thermomechanical applications. In contrast with gradient-type models, this strategy does not require additional equilibrium equations and boundary conditions. For the purpose of illustration, some numerical examples are presented. According to the numerical results, the proposed framework can be used to circumvent the difficulties associated with excessive spatial localization or to consider size effects.

Keywords Thermodynamics · Constitutive laws · Non-locality · Damage · Plasticity

1 Introduction

Many constitutive models used for thermo-mechanical applications rely on the internal variable concept [24] to represent the effect of microstructural transformations (*e.g.* hardening, damage, phase transitions) on the behavior of solid

C. Mareau
Arts et Metiers Institute of Technology, LAMPA, HESAM
2, boulevard du Ronceray
49035 Angers (France)
Tel.: +33-2-41207379
E-mail: charles.mareau@ensam.eu

materials. For the majority of constitutive models, the evolution equations associated with the different internal variables are purely local. Specifically, the evolution of the internal state of a material point solely depends on the current state of that material point. However, there are some situations for which it is needed to include some information regarding the spatial distribution of state variables. As discussed by Bažant and Jirásek [7], there are different motivations for such constitutive models, which are often referred to as non-local. Indeed, non-local models allow (i) considering deviations from locality due to material heterogeneity at small scales, (ii) limiting strain localization resulting from softening, which is largely used in the context of damage mechanics, and (iii) capturing size effects associated with metal plasticity [39,18] or fracture of ceramic materials [50,29].

Non-local constitutive models can be classified as either gradient-type or integral-type models[1]. Gradient-type models treat the spatial gradients of internal variables as additional state variables. The consequence is that the evolution of internal variables is governed by a set of equilibrium equations and some boundary conditions. Such equations and boundary conditions are generally derived from an extended principle of virtual power [22,14,36]. Gradient-type models have been largely used in the context of conventional plasticity, either to capture size effects [1,20] or to limit strain localization associated with softening [3]. Also, the role of Geometrically Necessary Dislocations (GND) on strain hardening can be incorporated in the framework of crystal plasticity by considering the spatial gradients of plastic shear strains as state variables [41,38,53]. The phase-field method, which is widely used for solving interfacial problems, also relies on the spatial gradients of some order parameters to evaluate surface energy. Many applications of the phase-field method to either brittle [34,42,10,25] or ductile fracture [28,2] have been proposed. When applied to fracture, the phase-field method allows circumventing the difficulties associated with excessive damage localization and considering the increase of surface energy resulting from crack nucleation and crack growth.

In contrast with gradient-type models, integral-type models use some non-local variables obtained after spatial integration of their local counterparts. Generally speaking, such non-local variables can be interpreted as the spatial averages of the corresponding local variables over the neighborhood of the material point of interest. Integral-type models have been largely used in the context of brittle [43,8,12] or ductile fracture [31,4], mostly to limit damage localization. Some alternative formulations, using either an evolving length scale [44] or an internal time [16], have been proposed to consider damage-dependent interactions. As discussed by [30], integral-type models for plasticity-induced softening have also been developed. For instance, Bažant and Lin [6] proposed a non-local Mohr-Coulomb model that replaces the local plastic strain tensor by its non-local counterpart. The approach of Polizzotto *et al.* [45], which is developed in a consistent thermodynamic framework, uses a non-local definition

[1] Gradient-type models are sometimes referred to as 'weakly' non-local models while integral models are referred to as 'strongly' non-local models [7].

of the isotropic hardening variable. In the context of crystal plasticity, Gao and Huang [23] and Counts *et al.* [15] developed a non-local formulation that accounts for the role of GND. For this purpose, they have used an integral-type of approach to evaluate the spatial gradient of the plastic deformation gradient tensor.

The present work aims at enriching integral-type constitutive models by incorporating not only the spatial average, but also the spatial variance of an internal variable in constitutive relations. The objective is to include additional information regarding the spatial distribution of an internal variable when constructing integral-type constitutive models. The proposed framework is developed in the context of continuum thermodynamics and can be applied to different types of problems, including plasticity and damage. In the first section, the definitions of the average and the variance of an internal variable are introduced. The general form of constitutive equations is detailed in the second section. Some illustrative examples are presented in the final section in either the context of damage mechanics, or crystal-plasticity.

2 Non-local internal variables

The development of constitutive relations, which is detailed in the next section, uses some internal variables to consider the impact of microstructural transformations on the state of a material point. The main idea of integral-type non-local models consists of assuming that the state of a material point (*e.g.* stress, internal energy) depends on the spatial distribution of state variables in its neighborhood. For this purpose, two different types of non-local variables are considered: the spatial average and the spatial variance. The definitions of these variables are briefly presented here.

2.1 Spatial average

Most integral-type models use some non-local variables that are obtained from the application of an averaging procedure. Specifically, for any local internal variable $\boldsymbol{\beta}$, the spatial average $\boldsymbol{\mu}_\beta$ is defined according to [11]:

$$\boldsymbol{\mu}_\beta[\boldsymbol{X}] = \frac{1}{W}\int_{\mathscr{V}_c} w[\boldsymbol{X}' - \boldsymbol{X}]\left(\boldsymbol{\beta}[\boldsymbol{X}'] - \boldsymbol{\beta}[\boldsymbol{X}]\right) d\boldsymbol{X}' + \boldsymbol{\beta}[\boldsymbol{X}] \tag{1}$$

As indicated by the above equation, the non-local variable $\boldsymbol{\mu}_\beta$ is actually the first raw moment associated with the spatial distribution of the local variable $\boldsymbol{\beta}$. The averaging procedure uses a weight function w that describes the interactions between material points with initial positions $\boldsymbol{X}$ and $\boldsymbol{X}'$. The region of space over which such interactions are considered is denoted by $\mathscr{V}_c$. The factor W is obtained by integrating the weight function over an infinite region of space $\mathscr{V}_\infty$, that is:

$$W = \int_{\mathscr{V}_\infty} w[\boldsymbol{X}']d\boldsymbol{X}' \tag{2}$$

For the development of constitutive relations, it may be needed to perform a double-averaging operation. For any internal variable $\boldsymbol{\beta}$, the corresponding double-averaged variable $\boldsymbol{\mu}_{\beta\beta}$ is given by:

$$\boldsymbol{\mu}_{\beta\beta}[\boldsymbol{X}] = \frac{1}{W}\int_{\mathscr{V}_c} w[\boldsymbol{X}' - \boldsymbol{X}]\left(\boldsymbol{\mu}_{\beta}[\boldsymbol{X}'] - \boldsymbol{\mu}_{\beta}[\boldsymbol{X}]\right) d\boldsymbol{X}' + \boldsymbol{\mu}_{\beta}[\boldsymbol{X}] \tag{3}$$

In some situations, it may be useful to construct a gradient approximation of the spatial average. For this purpose, the internal variable at position $\boldsymbol{X}'$ can be obtained from a Taylor series expansion at position $\boldsymbol{X}$ according to:

$$\boldsymbol{\beta}[\boldsymbol{X}'] = \boldsymbol{\beta}[\boldsymbol{X}] + \sum_k \frac{1}{k!}\left(\boldsymbol{X}' - \boldsymbol{X}\right)^{\otimes k} \bullet \left(\boldsymbol{\nabla}^{\otimes k} \otimes \boldsymbol{\beta}[\boldsymbol{X}]\right) \tag{4}$$

The above equation uses the following notations[2]:

$$\left(\boldsymbol{X}' - \boldsymbol{X}\right)^{\otimes k} \overset{\text{def}}{=} \underbrace{\left(\boldsymbol{X}' - \boldsymbol{X}\right) \otimes \cdots \otimes \left(\boldsymbol{X}' - \boldsymbol{X}\right)}_{k} \tag{5}$$

$$\nabla^{\otimes k} \otimes \boldsymbol{\beta} \overset{\text{def}}{=} \underbrace{\boldsymbol{\nabla} \otimes \cdots \otimes \boldsymbol{\nabla}}_{k} \otimes \boldsymbol{\beta} \tag{6}$$

Provided that the material point of interest is away from any internal or external boundary, the application of the averaging operator of Equation (1) is not impacted by spatial gradients of odd order. Also, when the interaction volume is small, the spatial average $\boldsymbol{\mu}_{\beta}$ can be approximated from the second order derivative of the internal variable $\boldsymbol{\beta}$ with:

$$\boldsymbol{\mu}_{\beta}[\boldsymbol{X}] \approx \boldsymbol{\beta}[\boldsymbol{X}] + \frac{1}{2}\boldsymbol{L} : \left(\boldsymbol{\nabla}^{\otimes 2} \otimes \boldsymbol{\beta}[\boldsymbol{X}]\right) \tag{7}$$

with:

$$\boldsymbol{L} = \frac{1}{W}\int_{\mathscr{V}_c} w[\boldsymbol{X}' - \boldsymbol{X}]\left(\boldsymbol{X}' - \boldsymbol{X}\right)^{\otimes 2} d\boldsymbol{X}' \tag{8}$$

The above approximation has been used by [49] and [13] to transform integral-type models into gradient-type models.

2.2 Spatial variance

When constructing constitutive relations, it might be necessary to provide additional information regarding the spatial distribution of an internal variable in the vicinity of a material point. For this purpose, higher order central moments of the internal variable $\boldsymbol{\beta}$ can be included in the list of state variables. In the following, our attention is restricted to the variance of the internal variable

[2] The notation $\boldsymbol{\nabla}$ is used to denote the derivative with respect to the initial position $\boldsymbol{X}$.

$\boldsymbol{\beta}$ (*i.e.* the second central moment). The spatial variance, which is denoted by $\boldsymbol{\xi}_\beta$, is obtained from:

$$\boldsymbol{\xi}_\beta[\boldsymbol{X}] = \frac{1}{W}\int_{\mathscr{V}_c} w[\boldsymbol{X}'-\boldsymbol{X}]\left(\left(\boldsymbol{\mu}_\beta[\boldsymbol{X}]-\boldsymbol{\beta}[\boldsymbol{X}']\right)^{\otimes 2}-\left(\boldsymbol{\mu}_\beta[\boldsymbol{X}]-\boldsymbol{\beta}[\boldsymbol{X}]\right)^{\otimes 2}\right)d\boldsymbol{X}' + \left(\boldsymbol{\mu}_\beta[\boldsymbol{X}]-\boldsymbol{\beta}[\boldsymbol{X}]\right)^{\otimes 2} \tag{9}$$

The spatial variance is a tensor whose rank is twice that of $\boldsymbol{\beta}$. It measures the scatter associated with the spatial distribution of the internal variable around the material point of interest.

The gradient approximation of the variance is obtained by combining Equations (4) and (9). Upon the condition that the point of interest is away from any internal or external boundary, the variance $\boldsymbol{\xi}_\beta$ can be approximated as a quadratic function of the first gradient of the local internal variable $\boldsymbol{\beta}$ with:

$$\boldsymbol{\xi}_\beta[\boldsymbol{X}] \approx (\boldsymbol{\beta}[\boldsymbol{X}]\otimes\boldsymbol{\nabla})\cdot\boldsymbol{L}\cdot(\boldsymbol{\nabla}\otimes\boldsymbol{\beta}[\boldsymbol{X}]) \tag{10}$$

This quadratic form is largely used in many gradient-type models (*e.g.* [21,52]). The above result indicates that such gradient-type models can be perceived as approximations of variance-based integral-type models.

2.3 Weight function

The weight function w, which is needed for the evaluation of non-local internal variables, allows controlling the mutual interactions between material points with initial positions $\boldsymbol{X}$ and $\boldsymbol{X}'$. The weight function is conveniently expressed as the composition of two functions k and r such that:

$$w[\boldsymbol{X}'-\boldsymbol{X}] = k\circ r[\boldsymbol{X}'-\boldsymbol{X}] \tag{11}$$

with:

$$r = \sqrt{(\boldsymbol{X}'-\boldsymbol{X})\cdot\boldsymbol{R}^{-2}\cdot(\boldsymbol{X}'-\boldsymbol{X})} \tag{12}$$

The symmetric and positive semi-definite second order tensor $\boldsymbol{R}$ is a material parameter that provides information regarding the distances and directions over which interactions are considered. Many theories use an isotropic weight function. For this specific case, the interaction tensor $\boldsymbol{R}$ is defined from an interaction radius R (with $R\geq 0$) according to:

$$\boldsymbol{R} = R\ \mathbf{1} \tag{13}$$

A more general definition consists of using an anisotropic weight function, in which case the interaction tensor $\boldsymbol{R}$ takes the following form:

$$\boldsymbol{R} = \sum_i R_i\ \boldsymbol{r}_i\otimes\boldsymbol{r}_i \tag{14}$$

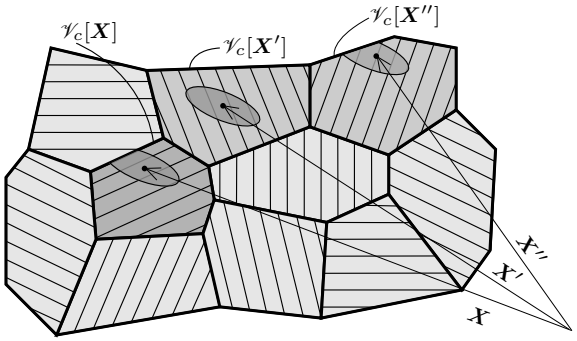

Fig. 1 Schematic diagram showing the interaction volume for different material points.

where the radii R_i and mutually orthogonal unit vectors $\boldsymbol{r}_i$ allow defining an interaction ellipsoid. It is worth mentioning that the choice of the interaction tensor $\boldsymbol{R}$ should comply with the restrictions due to material symmetry.

When the weight function w has bounded support, interactions are effective only in the region corresponding to the intersection of the interaction ellipsoid with the region $\mathscr{V}_c$ over which the internal variable is defined (see Figure 1). If the weight function w has unbounded support, interactions are effective within the entire definition domain of the internal variable $\mathscr{V}_c$. The underlying idea is that different constitutive models, with different sets of internal variables, may be used when modeling the thermomechanical behavior of a body. In such a case, only the material points for which the definition of the internal variable makes sense are considered when evaluating the non-local variable.

3 Field equations

In a thermomechanical context, the history of a material point with initial position $\boldsymbol{X}$ is described by the functions $\boldsymbol{\chi}$ and θ defining the motion and temperature histories. Such functions allow determining the current position $\boldsymbol{x}$ and absolute temperature T with:

$$\boldsymbol{x} = \boldsymbol{\chi}[\boldsymbol{X}, t] \text{ and } T = \theta[\boldsymbol{X}, t] \tag{15}$$

The evolution of the current position and temperature fields is governed by some partial differential equations, which are commonly classified as either conservation or constitutive equations. In the following, conservation equations are first briefly recalled. The general framework used for the construction of constitutive relations is then detailed.

3.1 Conservation equations

For a closed system, mass conservation requires that the initial mass density ϱ, which corresponds to the mass per unit volume in the initial configuration,

does not change with time [46]:

$$\dot{\varrho} = 0 \tag{16}$$

For linear and angular momenta to be conserved, the first Piola-Kirchoff stress tensor $\boldsymbol{P}$ must be such that:

$$\boldsymbol{P} \cdot \boldsymbol{\nabla} + \boldsymbol{B} = \varrho \ddot{\boldsymbol{x}} \tag{17}$$

$$\boldsymbol{P} \cdot \boldsymbol{F}^T = \boldsymbol{F} \cdot \boldsymbol{P}^T \tag{18}$$

where $\boldsymbol{F} = \partial \boldsymbol{x} / \partial \boldsymbol{X}$ is the deformation gradient tensor and $\boldsymbol{B}$ is the body force density.

Also, according to the first law of thermodynamics, the evolution of the specific internal energy e is given by:

$$\dot{e} = \frac{1}{\varrho} \boldsymbol{P} : \dot{\boldsymbol{F}} - \frac{1}{\varrho} \boldsymbol{\nabla} \cdot \boldsymbol{Q} + r_q + r_{nl} \tag{19}$$

where $\boldsymbol{Q}$ is the heat flux density vector and r_q is the specific heat supply. While the mass and momentum conservation equations display their classical form, it is important to mention that the local form of the first law of thermodynamics includes a non-conventional contribution that takes the form of a specific energy source r_{nl}. This additional energy source, which is sometimes referred to as the non-locality residual [45], results from the assumption of non-locality. Specifically, it represents the transfer of internal energy between interacting material points. For any material point, the specific source r_{nl} must satisfy the following condition:

$$\bar{r}_{nl}[\boldsymbol{X}] = \frac{1}{\mathscr{V}_c} \int_{\mathscr{V}_c} r_{nl}[\boldsymbol{X}'] d\boldsymbol{X}' = 0 \tag{20}$$

In the above equation, $\bar{r}_{nl}$ denotes the average value of the non-locality residual over the region $\mathscr{V}_c$, which corresponds to the domain over which the constitutive model is adopted (see Figure 1). In general, this region is not the volume occupied by the whole body. The condition (20) reflects the fact that a material point may transfer some internal energy to neighborhing material points but, when averaged over the volume $\mathscr{V}_c$, non-locality does not result in any net production or loss of energy. It is worth mentioning that the region over which the constitutive model is defined may coincide with the region occupied by the body of interest. For this specific but rather common situation, the average value of the non-locality residual $\bar{r}_{nl}$ is identical for all material points, hence does not depend on the initial position.

Finally, the second law of thermodynamics requires the specific entropy production source σ to be non-negative at any time and for any material point, which means that:

$$\sigma = \dot{s} + \frac{1}{\varrho} \boldsymbol{\nabla} \cdot \left(\frac{\boldsymbol{Q}}{T} \right) - \frac{r_q}{T} \geq 0 \tag{21}$$

where s is the specific entropy.

3.2 Constitutive equations

In a thermomechanical context, the list of state variables[3] used for the development of constitutive relations includes the deformation gradient tensor $\boldsymbol{F}$ and its rate $\dot{\boldsymbol{F}}$, the absolute temperature T, its spatial gradient $\boldsymbol{\nabla} T$, a local internal variable $\boldsymbol{\beta}$ and its non-local counterparts $\boldsymbol{\mu}_\beta$ and $\boldsymbol{\xi}_\beta$. The constitutive model consists of some constitutive relations for the first Piola-Kirchoff stress tensor $\boldsymbol{P}$, the heat flux density vector $\boldsymbol{Q}$, the specific free energy $a = e - sT$ and the specific entropy s. Such constitutive relations are formally written in the following form:

$$a = \hat{a}\left[\boldsymbol{F}, \dot{\boldsymbol{F}}, T, \boldsymbol{\nabla} T, \boldsymbol{\beta}, \boldsymbol{\mu}_\beta, \boldsymbol{\xi}_\beta\right] \tag{22}$$

$$s = \hat{s}\left[\boldsymbol{F}, \dot{\boldsymbol{F}}, T, \boldsymbol{\nabla} T, \boldsymbol{\beta}, \boldsymbol{\mu}_\beta, \boldsymbol{\xi}_\beta\right] \tag{23}$$

$$\boldsymbol{P} = \hat{\boldsymbol{P}}\left[\boldsymbol{F}, \dot{\boldsymbol{F}}, T, \boldsymbol{\nabla} T, \boldsymbol{\beta}, \boldsymbol{\mu}_\beta, \boldsymbol{\xi}_\beta\right] \tag{24}$$

$$\boldsymbol{Q} = \hat{\boldsymbol{Q}}\left[\boldsymbol{F}, \dot{\boldsymbol{F}}, T, \boldsymbol{\nabla} T, \boldsymbol{\beta}, \boldsymbol{\mu}_\beta, \boldsymbol{\xi}_\beta\right] \tag{25}$$

Also, when some internal variables are introduced, the corresponding evolution equations must also be included in the constitutive model. These equations allow describing how the microstructure of a material point is affected by a thermomechanical process. The evolution equations take the following form:

$$\dot{\boldsymbol{\beta}} = \hat{\boldsymbol{\beta}}\left[\boldsymbol{F}, \dot{\boldsymbol{F}}, T, \boldsymbol{\nabla} T, \boldsymbol{\beta}, \boldsymbol{\mu}_\beta, \boldsymbol{\xi}_\beta\right] \tag{26}$$

It is worth mentioning that no evolution equation is needed for non-local internal variables. Indeed, non-local internal variables are directly connected to their local counterparts with their definition given by either Equation (1) or Equation (9). Also, though the finite strain framework is used here for the purpose of generality, the proposed framework can be used in the infinitesimal strain context by considering the infinitesimal strain tensor (and its rate) as external state variables instead of the deformation gradient tensor (and its rate) in constitutive relations.

The specific dissipation source $d = \sigma T$, which must be non-negative, is obtained by combining the above equation with the energy conservation equation (19) and the definition of the specific free energy:

$$d = \frac{1}{\varrho}\boldsymbol{P} : \dot{\boldsymbol{F}} + r_{nl} - \dot{a} - s\dot{T} - \frac{1}{\varrho}\boldsymbol{\nabla} \ln[T] \cdot \boldsymbol{Q} \geq 0 \tag{27}$$

[3] For the purpose of conciseness, a single internal variable is considered here. The extension of the proposed framework for multiple internal variables is straightforward.

The specific free energy rate $\dot{a}$, which appears in the above inequality, is expressed as follows[4]:

$$\dot{a} = \frac{\partial a}{\partial \boldsymbol{F}} : \dot{\boldsymbol{F}} + \frac{\partial a}{\partial \dot{\boldsymbol{F}}} : \ddot{\boldsymbol{F}} + \frac{\partial a}{\partial T}\dot{T} + \frac{\partial a}{\partial \boldsymbol{\nabla} T} \cdot \boldsymbol{\nabla}\dot{T} + \frac{\partial a}{\partial \boldsymbol{\beta}} \bullet \dot{\boldsymbol{\beta}} + \frac{\partial a}{\partial \boldsymbol{\mu}_\beta} \bullet \dot{\boldsymbol{\mu}}_\beta + \frac{\partial a}{\partial \boldsymbol{\xi}_\beta} \blacksquare \dot{\boldsymbol{\xi}}_\beta \quad (28)$$

Using the above relation, the expression of the specific dissipation source becomes:

$$\begin{aligned} d = &\left(\frac{1}{\varrho}\boldsymbol{P} - \frac{\partial a}{\partial \boldsymbol{F}}\right) : \dot{\boldsymbol{F}} - \frac{\partial a}{\partial \dot{\boldsymbol{F}}} : \ddot{\boldsymbol{F}} - \left(s + \frac{\partial a}{\partial T}\right)\dot{T} - \frac{\partial a}{\partial \boldsymbol{\nabla} T} \cdot \boldsymbol{\nabla}\dot{T} \\ &- \frac{\partial a}{\partial \boldsymbol{\beta}} \bullet \dot{\boldsymbol{\beta}} - \frac{\partial a}{\partial \boldsymbol{\mu}_\beta} \bullet \dot{\boldsymbol{\mu}}_\beta - \frac{\partial a}{\partial \boldsymbol{\xi}_\beta} \blacksquare \dot{\boldsymbol{\xi}}_\beta + r_{nl} - \frac{1}{\varrho}\boldsymbol{\nabla} \ln[T] \cdot \boldsymbol{Q} \geq 0 \end{aligned} \quad (29)$$

The above inequality should hold for any temperature and motion history. Since the dissipation source exhibits a linear dependence with respect to $\ddot{\boldsymbol{F}}$, $\dot{T}$ and $\boldsymbol{\nabla}\dot{T}$, the specific free energy must satisfy the following conditions:

$$\frac{\partial a}{\partial \dot{\boldsymbol{F}}} = \boldsymbol{O},\ \frac{\partial a}{\partial T} = -s \text{ and } \frac{\partial a}{\partial \boldsymbol{\nabla} T} = \boldsymbol{0} \quad (30)$$

These conditions indicate that both the specific free energy and specific entropy should not depend on the deformation gradient rate and the temperature gradient, *i.e.*:

$$a = \hat{a}\left[\boldsymbol{F}, T, \boldsymbol{\beta}, \boldsymbol{\mu}_\beta, \boldsymbol{\xi}_\beta\right] \quad (31)$$

$$s = \hat{s}\left[\boldsymbol{F}, T, \boldsymbol{\beta}, \boldsymbol{\mu}_\beta, \boldsymbol{\xi}_\beta\right] \quad (32)$$

The dissipation inequality therefore takes the following form:

$$d = \frac{1}{\varrho}\boldsymbol{P}^{ir} : \dot{\boldsymbol{F}} + \frac{1}{\varrho}\boldsymbol{b} \bullet \dot{\boldsymbol{\beta}} + \frac{1}{\varrho}\boldsymbol{m} \bullet \dot{\boldsymbol{\mu}}_\beta + \frac{1}{\varrho}\boldsymbol{z} \blacksquare \dot{\boldsymbol{\xi}}_\beta + r_{nl} - \frac{1}{\varrho}\boldsymbol{\nabla} \ln[T] \cdot \boldsymbol{Q} \geq 0 \quad (33)$$

For the purpose of conciseness, the following quantities have been introduced:

$$\boldsymbol{P}^{ir} = \boldsymbol{P} - \varrho\frac{\partial a}{\partial \boldsymbol{F}} \quad (34)$$

$$\boldsymbol{b} = -\varrho\frac{\partial a}{\partial \boldsymbol{\beta}} \quad (35)$$

$$\boldsymbol{m} = -\varrho\frac{\partial a}{\partial \boldsymbol{\mu}_\beta} \quad (36)$$

$$\boldsymbol{z} = -\varrho\frac{\partial a}{\partial \boldsymbol{\xi}_\beta} \quad (37)$$

The dissipation inequality (33) does not allow constructing the evolution equation associated with the internal variable $\boldsymbol{\beta}$. Indeed, the contributions associated with the evolution of local and non-local internal variables are separated

[4] The inner product of two tensors whose rank is that of $\boldsymbol{\beta}$ (*e.g.* $\boldsymbol{\mu}_\beta$) is denoted by $\bullet$. In a similar fashion, the inner product of two tensors whose rank is twice that of $\boldsymbol{\beta}$ (*e.g.* $\boldsymbol{\xi}_\beta$) is denoted by $\blacksquare$.

though these variables are not independent from each other. To circumvent this difficulty, it is convenient to introduce the quantities $\boldsymbol{\mu}_m$, $\boldsymbol{\mu}_z$ and $\boldsymbol{\mu}_x$ such that (see Appendix A):

$$\overline{\boldsymbol{m} \bullet \dot{\boldsymbol{\mu}}_\beta} = \overline{\boldsymbol{\mu}_m \bullet \dot{\boldsymbol{\beta}}} \tag{38}$$

$$\overline{\boldsymbol{z} \blacksquare \dot{\boldsymbol{\xi}}_\beta} = \overline{2\left(\boldsymbol{\mu}_z \bullet \boldsymbol{\beta} - \boldsymbol{\mu}_x\right) \bullet \dot{\boldsymbol{\beta}}} \tag{39}$$

To satisfy the above averaging conditions, the quantities $\boldsymbol{\mu}_m$, $\boldsymbol{\mu}_z$ and $\boldsymbol{\mu}_x$ are defined according to:

$$\boldsymbol{\mu}_m[\boldsymbol{X}] = \frac{1}{W}\int_{\mathscr{V}_c} w[\boldsymbol{X}' - \boldsymbol{X}]\left(\boldsymbol{m}[\boldsymbol{X}'] - \boldsymbol{m}[\boldsymbol{X}]\right) d\boldsymbol{X}' + \boldsymbol{m}[\boldsymbol{X}] \tag{40}$$

$$\boldsymbol{\mu}_z[\boldsymbol{X}] = \frac{1}{W}\int_{\mathscr{V}_c} w[\boldsymbol{X}' - \boldsymbol{X}]\left(\boldsymbol{z}[\boldsymbol{X}'] - \boldsymbol{z}[\boldsymbol{X}]\right) d\boldsymbol{X}' + \boldsymbol{z}[\boldsymbol{X}] \tag{41}$$

$$\begin{aligned}\boldsymbol{\mu}_x[\boldsymbol{X}] = \frac{1}{W}\int_{\mathscr{V}_c} w[\boldsymbol{X}' - \boldsymbol{X}]\left(\boldsymbol{z}[\boldsymbol{X}'] \bullet \boldsymbol{\mu}_\beta[\boldsymbol{X}'] - \boldsymbol{z}[\boldsymbol{X}] \bullet \boldsymbol{\mu}_\beta[\boldsymbol{X}]\right) d\boldsymbol{X}' \\ + \boldsymbol{z}[\boldsymbol{X}] \bullet \boldsymbol{\mu}_\beta[\boldsymbol{X}]\end{aligned} \tag{42}$$

Using the properties (38) and (39), the dissipation inequality is rewritten as:

$$d = \frac{1}{\varrho}\boldsymbol{P}^{ir} : \dot{\boldsymbol{F}} + \frac{1}{\varrho}\boldsymbol{B} \bullet \dot{\boldsymbol{\beta}} - \frac{1}{\varrho}\boldsymbol{\nabla}\ln[T] \cdot \boldsymbol{Q} \geq 0 \tag{43}$$

with:

$$\boldsymbol{B} = \boldsymbol{b} + \boldsymbol{\mu}_m + 2\boldsymbol{\mu}_z \bullet \boldsymbol{\beta} - 2\boldsymbol{\mu}_x \tag{44}$$

The above equation indicates that the dissipative force $\boldsymbol{B}$ driving the evolution of the internal variable $\boldsymbol{\beta}$ includes a local contribution as well as some non-local contributions resulting from the introduction of the spatial average and spatial variance in the list of state variables. Also, to obtain the above dissipation inequality, the following definition of the specific energy source r_{nl} has been adopted:

$$r_{nl} = \boldsymbol{m} \bullet \dot{\boldsymbol{\mu}}_\beta + \boldsymbol{z} \blacksquare \dot{\boldsymbol{\xi}}_\beta - \boldsymbol{\mu}_m \bullet \dot{\boldsymbol{\beta}} - 2\left(\boldsymbol{\mu}_z \bullet \boldsymbol{\beta} - \boldsymbol{\mu}_x\right) \bullet \dot{\boldsymbol{\beta}} \tag{45}$$

Because of the equalities (38) and (39), the condition (20) is automatically fulfilled for any material point and at any time for the body of interest. The dissipation inequality (43) is the starting point for the construction of evolution equations. Indeed, it indicates that the evolution of the state of a material point is controlled by the dissipative forces $\boldsymbol{P}^{ir}$, $\boldsymbol{B}$ and $\boldsymbol{\nabla}\ln[T]$. In contrast with conventional (*i.e.* local) theories, the evolution of the internal variable $\boldsymbol{\beta}$ is driven by the dissipative force $\boldsymbol{B}$ that includes both local and non-local contributions when the proposed framework is adopted.

4 Numerical examples

For illustration purposes, some numerical examples using the proposed framework are presented in this section. Such examples aim at showing the possible advantages offered by the introduction of higher order non-local internal variables when constructing constitutive models for thermomechanical applications.

The following examples deal with crystalline materials. In the following, an isotropic interaction tensor (see Equation (13)) is used whatever the crystal structure is, mostly for simplicity reasons. The underlying assumption is that the interactions between different material points only depend on their relative distance. The function r therefore takes the following form:

$$r[\boldsymbol{X}' - \boldsymbol{X}] = \frac{||\boldsymbol{X}' - \boldsymbol{X}||}{R} \tag{46}$$

Also, a biquadratic function is used for k, that is[5]:

$$k[r] = \frac{15}{16}\langle 1 - r^2 \rangle_+^2 \tag{47}$$

To solve the differential equations resulting from static equilibrium and compatibility, the spectral method [35] is used. This method allows evaluating the behavior of a volume element with periodic boundary conditions. The spectral method has been implemented in the context of finite strains according to the iterative procedure presented by Eisenlohr *et al.* [17]. The sole modification concerns the evaluation of non-local internal variables. Specifically, non-local variables are obtained from their local counterparts once constitutive relations have been integrated from a discrete convolution operation. Non-local variables are then used as an input for the integration of constitutive relations during the next iteration. This procedure is repeated until convergence is achieved. Also, for simplicity, the temperature field is assumed to be uniform and constant, which corresponds to the specific case of isothermal conditions.

4.1 Example 1: Damage localization

Constitutive relations For the present application, the construction of constitutive relations relies on the general framework of continuum damage mechanics [32]. Specifically, a scalar internal variable β is introduced to represent the degradation of mechanical resistance of a material point. The damage variable is equal to one for a fully damaged material point. At the opposite, a zero value corresponds to the absence of damage. Assuming that fracture is controlled by brittle damage, the specific free energy a is decomposed into three contributions according to:

$$a = a_e + a_d + a_{th} \tag{48}$$

[5] The positive part of a variable (say x) is given by $\langle x \rangle_+ = (x + |x|)/2$.

The elastic strain energy contribution a_e is given by:

$$a_e = \frac{1}{2\varrho} \boldsymbol{E} : \mathbb{C} : \boldsymbol{E} \tag{49}$$

where $\mathbb{C}$ is the stiffness tensor and $\boldsymbol{E}$ is the Green strain tensor:

$$\boldsymbol{E} = \frac{1}{2}\left(\boldsymbol{F}^T \cdot \boldsymbol{F} - \mathbf{1}\right) \tag{50}$$

To consider closure effects, the impact of damage on stiffness properties is described according to:

$$\mathbb{C} = \begin{cases} (1-\beta)\ \mathbb{C}_0 & \text{if } \mathrm{tr}[\boldsymbol{E}] > 0 \\ (1-\beta)\ \mathbb{C}_0 + \beta\ \mathbb{P}_s : \mathbb{C}_0 : \mathbb{P}_s & \text{if } \mathrm{tr}[\boldsymbol{E}] \leq 0 \end{cases} \tag{51}$$

where $\mathbb{C}_0$ is the initial stiffness tensor. The above equation assumes that the spherical contribution to the stiffness tensor is recovered when the spherical strain is negative. For this purpose, Equation (51) uses the spherical projection tensor $\mathbb{P}_s$ given by:

$$\mathbb{P}_s = \frac{1}{3}\mathbf{1} \otimes \mathbf{1} \tag{52}$$

For the contribution of damage to free energy a_d, different options (a-d) are explored:

$$a_d = \frac{1}{\varrho} A \left(2\beta - \beta^2\right) \tag{53a}$$

$$a_d = \frac{1}{\varrho} A \left(2\beta - \beta^2\right) + \frac{1}{\varrho}\ \frac{G}{2} \left(\beta - \mu_\beta\right)^2 \tag{53b}$$

$$a_d = \frac{1}{\varrho} A \left(2\beta - \beta^2\right) + \frac{1}{\varrho}\ \frac{G}{2} \left(\left(\beta - \mu_\beta\right)^2 + \xi_\beta\right) \tag{53c}$$

$$a_d = \frac{1}{\varrho} A \left(2\beta - \beta^2\right) + \frac{1}{\varrho}\ \frac{G}{2} \xi_\beta \tag{53d}$$

In the above equations, A and G are material parameters controlling respectively the local and non-local contributions of damage to free energy. While the local contribution takes the form suggested by Wu [51], different propositions regarding the non-local contribution are considered. The first option (a) corresponds to a purely local damage model. For the other options (b-d), the non-local contribution, which vanishes for a uniform damage field, is estimated from the spatial average μ_β and/or the spatial variance ξ_β of the damage variable. The case where the spatial average is the sole non-local internal variable (b) corresponds to the standard non-local approach. The options involving the spatial variance (c and d), alone or together with the spatial average, are presented to demonstrate the possibilities offered by the proposed framework. From a thermodynamic point of view, it is worth mentioning that, in comparison with the local model (a), an affine distribution of the damage variable leads to an increase of free energy for variance-based models (c or d). At the

opposite, an affine distribution of the damage variable does not provide any additional contribution to free energy when the standard average-based model (b) is adopted.

The thermal contribution to free energy, which is denoted by a_{th}, does not need to be specified because isothermal conditions are assumed.

The state equations are established by differentiating the specific free energy with respect to the different state variables. In the absence of viscous contribution to the stress state (*i.e.* $\boldsymbol{P}^{ir} = \boldsymbol{O}$), the first Piola-Kirchoff stress tensor is:

$$\boldsymbol{P} = \varrho \frac{\partial a}{\partial \boldsymbol{F}} = \boldsymbol{F} \cdot (\mathbb{C} : \boldsymbol{E}) \tag{54}$$

The differentiation of free energy with respect to the damage variable leads to the expression of the energy restitution rate b:

$$b = -\varrho \frac{\partial a}{\partial \beta} = -\frac{1}{2}\boldsymbol{E} : \frac{\partial \mathbb{C}}{\partial \beta} : \boldsymbol{E} + 2A\,(\beta - 1) \tag{55a or 55d}$$

$$b = -\varrho \frac{\partial a}{\partial \beta} = -\frac{1}{2}\boldsymbol{E} : \frac{\partial \mathbb{C}}{\partial \beta} : \boldsymbol{E} + 2A\,(\beta - 1) + G\,(\mu_\beta - \beta) \tag{55b or 55c}$$

The driving force associated with the spatial average of the damage variable is given by:

$$m = -\varrho \frac{\partial a}{\partial \mu_\beta} = 0 \tag{56a or 56d}$$

$$m = -\varrho \frac{\partial a}{\partial \mu_\beta} = G\,(\beta - \mu_\beta) \tag{56b or 56c}$$

In a similar fashion, the driving force associated with the spatial variance is:

$$z = -\varrho \frac{\partial a}{\partial \xi_\beta} = 0 \tag{57a or 57b}$$

$$z = -\varrho \frac{\partial a}{\partial \xi_\beta} = -\frac{G}{2} \tag{57c or 57d}$$

Using the above state equations, the dissipation equality reduces to:

$$d = \frac{1}{\varrho} B \dot{\beta} - \frac{1}{\varrho} \boldsymbol{\nabla} \ln[T] \cdot \boldsymbol{Q} \geq 0 \tag{58}$$

with:

$$B = -\frac{1}{2}\boldsymbol{E} : \frac{\partial \mathbb{C}}{\partial \beta} : \boldsymbol{E} + 2A\,(\beta - 1) \tag{59a}$$

$$B = -\frac{1}{2}\boldsymbol{E} : \frac{\partial \mathbb{C}}{\partial \beta} : \boldsymbol{E} + 2A\,(\beta - 1) + G\,(2\mu_\beta - \beta - \mu_{\beta\beta}) \tag{59b}$$

$$B = -\frac{1}{2}\boldsymbol{E} : \frac{\partial \mathbb{C}}{\partial \beta} : \boldsymbol{E} + 2A\,(\beta - 1) + 2G\,(\mu_\beta - \beta) \tag{59c}$$

$$B = -\frac{1}{2}\boldsymbol{E} : \frac{\partial \mathbb{C}}{\partial \beta} : \boldsymbol{E} + 2A\,(\beta - 1) + G\,(\mu_{\beta\beta} - \beta) \tag{59d}$$

When the formulation is purely local (a), the dissipative force driving the development of damage does not contain any contribution limiting damage localization. For the models that use the spatial variance (c and d), the non-local contribution to the dissipative force has a clear meaning. Whatever the damage field is, the non-local contribution participates in damage diffusion by reducing the difference between the damage variable β and its spatial (single or double) average (μ_β or $\mu_{\beta\beta}$). This non-local contribution can therefore be interpreted as a localization limiter. For the standard non-local approach (b), which considers the damage variable and its spatial average as internal variables, the non-local contribution also promotes damage diffusion. This non-local contribution tends to reduce the difference between the local damage variable β and a non-local variable ($2\mu_\beta - \mu_{\beta\beta}$).

From a computational perspective, the mixed model (c), which uses both the variance and the average, requires less computational efforts than the standard non-local approach (b). Indeed, for the evaluation of the non-local contribution to the dissipative force, only one averaging operation needs to be performed. At the opposite, when the standard non-local approach (b) is adopted, both the single and the double-averaging operations must be applied to the damage variable to evaluate the non-local contribution to the dissipative force driving damage development.

In the context of standard materials, the evolution equations associated with the damage variable and the heat flux density vector are derived from a dissipation potential. Because of the restriction to isothermal conditions, the constitutive equation for the heat flux vector does not need to be established here. The dependence of the dissipation potential to the temperature logarithm gradient is therefore ignored. In the present case, the dissipation potential ϕ displays the following form:

$$\phi = \frac{K}{2\varrho}\left(\frac{\langle B\rangle_+}{K}\right)^2 (1-\beta) \tag{60}$$

where K is a viscosity parameter. The differentiation of the dissipation potential with respect to the dissipative force B leads to the following evolution equation for the damage variable:

$$\dot{\beta} = \varrho\frac{\partial \phi}{\partial B} = \frac{\langle B\rangle_+}{K}(1-\beta) \tag{61}$$

It is worth mentioning that the above evolution equation only allows damage growth (*i.e.* healing is not allowed).

Parameters and loading conditions The volume element used for this application is shown in Figure 2. It is composed of 64 equiaxed randomly oriented grains, with an average grain size of 25 μm. To evaluate the impact of spatial discretization on numerical results, resolutions ranging from 32^3 to 128^3 voxels have been used for the application of the spectral method. Since the size of the volume element is 100 μm, the voxel size ranges from 1.6 μm to 0.5

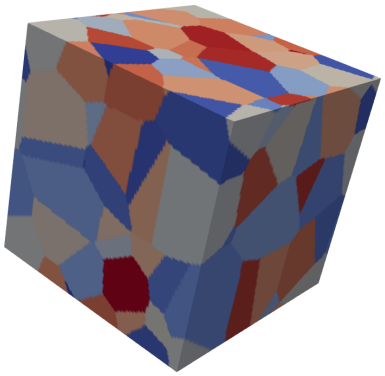

Fig. 2 Polycrystalline volume element used for the application of the spectral method.

Table 1 Material parameters for the brittle damage model. The Laue class corresponding to the crystalline solid is 6/mmm (hexagonal system). Only independent elastic constants are given.

Stiffness				
$\mathbb{C}_{1111}$	$\mathbb{C}_{1122}$	$\mathbb{C}_{3333}$	$\mathbb{C}_{1133}$	$\mathbb{C}_{1212}$
163.7 GPa	36.4 GPa	63.5 GPa	53.0 GPa	38.8 GPa
Damage			Radius	
A	G	K	R	
10^{-1} MPa	1 MPa	5×10^{-3} MPa.s	2 μm	

μm. Also, to investigate the development of brittle damage, periodic boundary conditions corresponding to uniaxial tension with a constant axial strain rate of 10^{-3} s^{-1} are prescribed to the volume element.

The material parameters used for the numerical simulations are listed in Table 1. An interaction radius R of 2 μm is used for the computation of non-local damage variables.

Results The evolution of the macroscopic axial stress as a function of the macroscopic axial strain obtained for a resolution of 128^3 is plotted in Figure 3. The macroscopic behavior is qualitatively similar for the different models. Specifically, the axial stress first increases and drops rapidly when damage develops significantly. When the formulation is purely local, the maximum axial stress is lower than that obtained with non-local models. Indeed, when the non-local contribution is adopted, the development of damage is accompanied by a diffusion process that reduces the impact of the singularities resulting from damage development.

The total dissipated energy and peak stress are plotted as a function of resolution in Figure 4. According to the numerical results, some differences exist regarding mesh dependency. Specifically, in contrast with non-local formulations (b-d), the results obtained with the local formulation (a) strongly depend on mesh resolution. This difference is attributed to the localization of damage within a few voxels. Strong spatial damage localization, hence mesh dependency, is largely reduced when non-locality is introduced. This is particularly

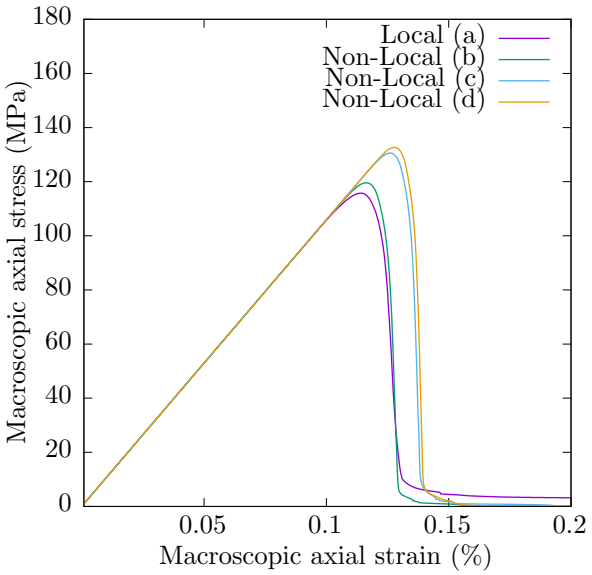

Fig. 3 Stress-strain diagrams obtained for a uniaxial tension test with the different damage models.

true for variance-based models (c or d) that exhibit the lowest dependency with respect to mesh resolution. The difference with the average-based model (b) is attributed to the fact that the non-local contribution to the dissipative force, which drives damage diffusion, is higher when the spatial variance is introduced.

4.2 Example 2: Polycrystalline plasticity

Constitutive relations To describe the elastic-viscoplastic behavior of a crystalline material point, the deformation gradient tensor is decomposed into elastic (superscript e) and plastic (superscript p) contributions according to:

$$\boldsymbol{F} = \boldsymbol{F}_e \cdot \boldsymbol{F}_p \tag{62}$$

In addition to the plastic contribution to the deformation gradient tensor $\boldsymbol{F}_p$, the list of internal state variables used for the present constitutive model includes some isotropic hardening variables. In the following, the hardening variable attached to the sth slip system is denoted by β^s and the corresponding spatial average and variance are respectively denoted by μ_β^s and ξ_β^s. The proposed model is similar in spirit to the non-local softening plasticity models of Vermeer and Brinkgreve [48] and Strömberg and Ristinmaa [47] in the sense that non-locality is introduced *via* isotropic hardening variables. This approach contrasts with common strain gradient plasticity models (*e.g.* [1],[53])

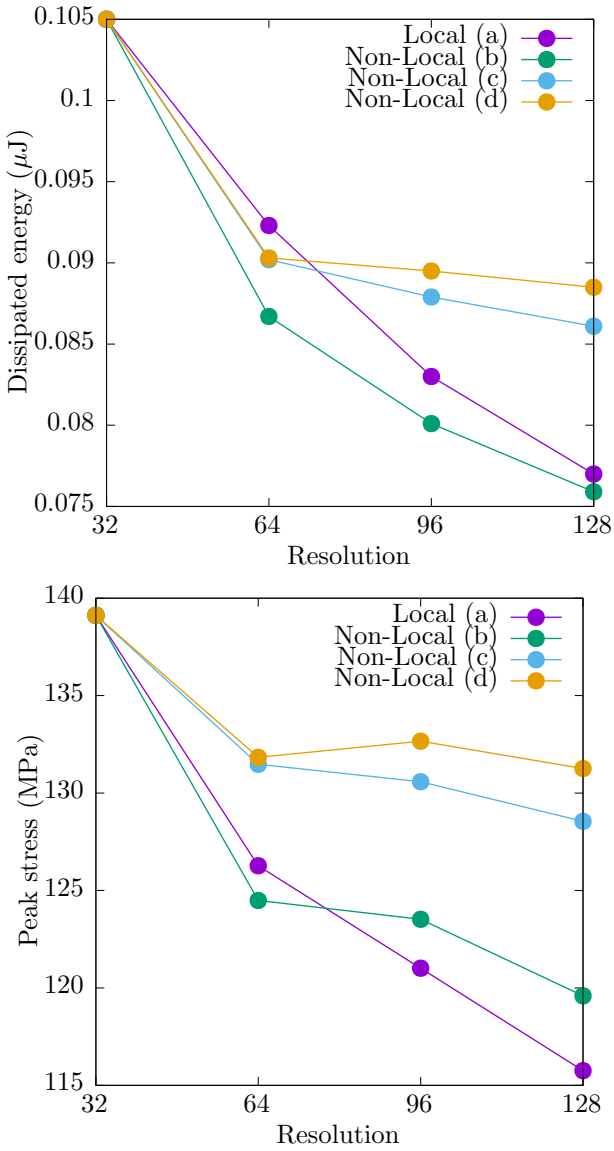

Fig. 4 Evolution of the total dissipated energy (top) and peak stress (bottom) as a function of the mesh resolution.

that consider the spatial gradients of plastic strains, rather than hardening variables.

The proposed set of state variables allows decomposing the specific free energy a into three contributions corresponding to elastic strain energy a_e,

defect energy a_d and thermal energy a_{th} such that:

$$a = a_e + a_d + a_{th} \tag{63}$$

The elastic contribution to free energy is given by:

$$a_e = \frac{1}{2\varrho} \boldsymbol{E}^e : \mathbb{C} : \boldsymbol{E}^e \tag{64}$$

where $\mathbb{C}$ is the stiffness tensor and $\boldsymbol{E}_e$ is the elastic Green strain tensor:

$$\boldsymbol{E}_e = \frac{1}{2}\left(\boldsymbol{F}_e^T \cdot \boldsymbol{F}_e - \boldsymbol{1}\right) \tag{65}$$

As for the damage model, different options (a-d) are explored for the contribution of defects to free energy:

$$a_d = \frac{1}{2\varrho} \sum_s \beta^s \sum_t H^{st} \beta^t \tag{66a}$$

$$a_d = \frac{1}{2\varrho} \sum_s \beta^s \sum_t H^{st} \beta^t + \frac{1}{2\varrho} G \sum_s (\beta^s - \mu_\beta^s)^2 \tag{66b}$$

$$a_d = \frac{1}{2\varrho} \sum_s \beta^s \sum_t H^{st} \beta^t + \frac{1}{2\varrho} G \sum_s \left((\beta^s - \mu_\beta^s)^2 + \xi_\beta^s\right) \tag{66c}$$

$$a_d = \frac{1}{2\varrho} \sum_s \beta^s \sum_t H^{st} \beta^t + \frac{1}{2\varrho} G \sum_s \xi_\beta^s \tag{66d}$$

In the above equation, H is the isotropic hardening matrix and G is a material parameter controlling the non-local contribution to free energy. The first option (a) corresponds to a purely local formulation while the other options (b-d) are non-local. For the latter formulations, the non-local contribution is either evaluated from the spatial averages (b and c) and/or the spatial variance (c and d) of the isotropic hardening variables.

Since isothermal conditions are considered, the thermal contribution to free energy, which solely depends on temperature, does not need to be specified.

In the absence of viscous stress, the first Piola-Kirchoff stress tensor is given by:

$$\boldsymbol{P} = \varrho \frac{\partial a}{\partial \boldsymbol{F}} \tag{67}$$

$$= \boldsymbol{F}_e \cdot (\mathbb{C} : \boldsymbol{E}_e) \cdot \boldsymbol{F}_p^{-T} \tag{68}$$

Depending on the retained option, one obtains the following state equations for the driving force associated with the hardening variable for the sth system:

$$b^s = -\varrho \frac{\partial a}{\partial \beta^s} = -\sum_t H^{st} \beta^t \tag{69a or 69d}$$

$$b^s = -\varrho \frac{\partial a}{\partial \beta^s} = -\sum_t H^{st} + G(\mu_\beta^s - \beta^s) \tag{69b or 69c}$$

For each slip system s, the driving force associated with the spatial average of the hardening variable is:

$$m^s = -\varrho \frac{\partial a}{\partial \mu^s_\beta} = 0 \tag{70a or 70d}$$

$$m^s = -\varrho \frac{\partial a}{\partial \mu^s_\beta} = G(\beta^s - \mu^s_\beta) \tag{70b or 70c}$$

For the spatial variance of the hardening variable, the corresponding driving force is given by:

$$z^s = -\varrho \frac{\partial a}{\partial \xi^s_\beta} = 0 \tag{71a or 71b}$$

$$z^s = -\varrho \frac{\partial a}{\partial \xi^s_\beta} = -\frac{G}{2} \tag{71c or 71d}$$

Using the proposed framework, the expression of the specific dissipation source d reduces to:

$$d = \frac{1}{\varrho} \boldsymbol{\Sigma} : \boldsymbol{L}_p + \frac{1}{\varrho} \sum_s B^s \dot{\beta}^s - \frac{1}{\varrho} \boldsymbol{\nabla} \ln T \cdot \boldsymbol{Q} \tag{72}$$

where $\boldsymbol{L}_p = \dot{\boldsymbol{F}}_p \cdot \boldsymbol{F}_p^{-1}$ is the plastic contribution to the velocity gradient. The above equation indicates that plastic flow is controlled by the Mandel stress tensor $\boldsymbol{\Sigma}$ [33], whose expression is:

$$\boldsymbol{\Sigma} = \boldsymbol{F}_e^T \cdot \boldsymbol{P} \cdot \boldsymbol{F}_p^T \tag{73}$$

The stress-like quantity B^s is the conjugate force to the hardening variable β^s. The application of relation (44) leads to:

$$B^s = -\sum_t H^{st} \beta^t \tag{74a}$$

$$B^s = G\left(2\mu^s_\beta - \mu^s_{\beta\beta} - \beta^s\right) - \sum_t H^{st} \beta^t \tag{74b}$$

$$B^s = 2G\left(\mu^s_\beta - \beta^s\right) - \sum_t H^{st} \beta^t \tag{74c}$$

$$B^s = G\left(\mu^s_{\beta\beta} - \beta^s\right) - \sum_t H^{st} \beta^t \tag{74d}$$

In the context of crystal plasticity, each slip system s is defined from two unit vectors: the slip plane normal $\boldsymbol{n}^s$ and the slip direction $\boldsymbol{m}^s$. When plastic flow is the sole result of crystallographic slip, the plastic contribution to the velocity gradient $\boldsymbol{L}_p$ is obtained from:

$$\boldsymbol{L}_p = \sum_s \boldsymbol{m}^s \otimes \boldsymbol{n}^s \nu^s \tag{75}$$

where ν^s is the plastic shear strain rate for each slip system. To consider the size-dependence of the hardening rate, the critical resolved shear stress r^s, which represents the resistance to plastic flow for the sth slip system, is defined according to:

$$r^s = -B^s \tag{76a}$$

$$r^s = -B^s\sqrt{1 + L\sqrt{(\beta^s - \mu^s_\beta)^2}} \tag{76b}$$

$$r^s = -B^s\sqrt{1 + L\sqrt{(\beta^s - \mu^s_\beta)^2 + \xi^s_\beta}} \tag{76c}$$

$$r^s = -B^s\sqrt{1 + L\sqrt{\xi^s_\beta}} \tag{76d}$$

where L is a material parameter. In contrast with local crystal-plasticity based models (a), the resistance to plastic flow includes a non-local contribution (b-d) that results from inhomogeneous hardening. Such a contribution vanishes when the hardening variable is (at least locally) uniformly distributed, in which case the linear isotropic hardening rule is retrieved. To determine whether the conditions for plastic flow are met or not, it is convenient to introduce a yield function f^s for each slip system s such that:

$$f^s = |\tau^s| - r^s \tag{77}$$

with:

$$\tau^s = \boldsymbol{m}^s \cdot \boldsymbol{\Sigma} \cdot \boldsymbol{n}^s \tag{78}$$

The dissipation potential ϕ used to obtain the evolution equations takes the following form:

$$\phi = \frac{1}{\varrho}\sum_s \frac{K}{M+1}\left(\frac{\langle f^s\rangle}{K}\right)^{M+1} \tag{79}$$

where K and M are some viscosity parameters. The plastic shear strain rate is thus given for each slip system s by:

$$\nu^s = \varrho\frac{\partial\phi}{\partial\tau^s} = \left(\frac{\langle f^s\rangle}{K}\right)^M \operatorname{sign}\left[\tau^s\right] \tag{80}$$

Also, the evolution equations for the hardening variables obtained for the different options are:

$$\dot\beta^s = \varrho\frac{\partial\phi}{\partial B^s} = -\varrho\frac{\partial\phi}{\partial r^s}\frac{\partial r^s}{\partial B^s} = |\nu^s| \tag{81a}$$

$$\dot\beta^s = \varrho\frac{\partial\phi}{\partial B^s} = -\varrho\frac{\partial\phi}{\partial r^s}\frac{\partial r^s}{\partial B^s} = |\nu^s|\sqrt{1 + L\sqrt{(\beta^s - \mu^s_\beta)^2}} \tag{81b}$$

$$\dot\beta^s = \varrho\frac{\partial\phi}{\partial B^s} = -\varrho\frac{\partial\phi}{\partial r^s}\frac{\partial r^s}{\partial B^s} = |\nu^s|\sqrt{1 + L\sqrt{(\beta^s - \mu^s_\beta)^2 + \xi^s_\beta}} \tag{81c}$$

$$\dot\beta^s = \varrho\frac{\partial\phi}{\partial B^s} = -\varrho\frac{\partial\phi}{\partial r^s}\frac{\partial r^s}{\partial B^s} = |\nu^s|\sqrt{1 + L\sqrt{\xi^s_\beta}} \tag{81d}$$

Table 2 Material parameters for the crystal plasticity model. The Laue class corresponding to the crystalline solid is m$\bar{3}$m (cubic system). Only independent elastic constants are given.

	Stiffness		Viscoplasticity	
$\mathbb{C}_{1111}$	$\mathbb{C}_{1122}$	$\mathbb{C}_{1212}$	K	M
168.3 GPa	122.1 GPa	75.7 GPa	10 MPa	20
	Hardening			Radius
H_{ss}	H_{st}	G	L	R
200 MPa	200 MPa	10 GPa	1000	2 μm

Parameters and loading conditions The volume element used to investigate the elasto-plastic behavior is the same as for the previous example (see Figure 2). To study size effects, three different grain sizes have been considered: 12.5 μm, 25 μm and 50 μm. The results obtained for an infinite grain size, which correspond to the local formulation, are also provided. The boundary conditions prescribed to the volume element correspond to a simple shear test with a constant shear strain rate of 10^{-2} s^{-1}. The material parameters used for performing the numerical simulations are listed in Table 2. For the present application, the hardening variables have an initial value of 1.25%, which corresponds to an initial critical resolved shear stress of 30 MPa.

Results The evolution of the macroscopic tangential stress as a function of the macroscopic shear strain is plotted in Figure 5 for the different grain sizes. According to the numerical results, the reduction of grain size leads to an increase of both the yield stress and the hardening rate. In the present context, this size effect is attributed to the inhomogeneous distribution of the hardening variable, which affects the resistance to plastic flow. It is worth noticing that, in comparison with the average-based model (b), the impact of grain size on the elasto-plastic behavior is more significant when the spatial variance (c or d) is introduced. Since the spatial average does not much contribute to size effects, the mixed (c) and variance-based (d) models provide similar results.

The yield stress obtained from the non-local models (b, c or d) is plotted as a function of the inverse of the square root of the average grain size in Figure 6. According to the results, the yield stress tends toward a minimum value when the grain size approaches infinity, which is consistent with the Hall-Petch equation. This effect is due to the fact that the non-local contribution to hardening is negligible for large grain sizes. When the grain size is reduced, the dependence of the yield stress with respect to the average grain size is close to that given by the Hall-Petch equation when either the mixed (c) or variance-based (d) models are adopted. While the results obtained with the average-based model (b) are size-dependent, the role of grain size on the development of plasticity is not fully consistent with the Hall-Petch equation. Such results highlight the possible benefits of considering the spatial variance of hardening variables in the description of size effects.

It should be mentioned that, in contrast with gradient-type models (*e.g.* [27],[9]), integral-type models are not well suited for very small grain sizes, *i.e.* inferior to the interaction radius R. Indeed, when the interaction volume

is large in comparison with the grain size, the spatial average and spatial variance reach asymptotic values in the sense that they are not much affected by further grain size reduction. As a result, the impact of grain size on the yield stress is not correctly depicted for very small grain sizes. Additional developments are therefore needed to improve the description of size effects over a wide range of grain sizes with (average- or variance-based) integral-type models.

The spatial distribution of the cumulated plastic strain $\beta_{eq} = \sum_s \beta^s$ obtained at the end of the shear test with the variance-based model (d) is shown in Figure 7 for different grain sizes. Plastic strain localization is less pronounced for the finest microstructure due to non-local effects. At the opposite, for the coarsest microstructure, significant plastic strains have been accumulated near grain boundaries as a result of internal stresses. In this latter case, non-local effects have a negligible impact on the spatial distribution of plastic deformation. The norm of $\boldsymbol{\nabla} \times \boldsymbol{F}_p$, which provides a quantitative measure of plastic deformation incompatibility, is also plotted in Figure 8 for the different grain sizes. This quantity is related to the density of GND [5]. According to the results, though the proposed model does not explicitly use GND densities, the reduction of grain size leads to higher plastic deformation incompatibilities, hence higher GND densities. Also, GND preferably accumulate near grain boundaries, which are the regions where significant plastic deformation incompatibilities are observed.

To illustrate the energetic implications of the present model, the evolution of the average internal energy density as a function of the macroscopic shear strain is plotted in Figure 9 for the variance-based model (d). According to the results, the grain size reduction leads to an increase of internal energy that is attributed to heterogeneous hardening.

5 Conclusions

In the present work, a general framework has been proposed to construct variance-based non-local constitutive models. In contrast with most integral-type constitutive models, which only use the spatial averages, the spatial variances of internal variables are treated as additional state variables. The proposed framework relies on continuum thermodynamics to construct the state equations and the evolution equations, which incorporate some non-local contributions. Such contributions allow considering the impact of the spatial distribution of internal variables on the thermomechanical behavior of solid materials without introducing additional equilibrium equations and boundary conditions. For the purpose of illustration, some numerical examples have been presented. According to the numerical results, the proposed framework can be used to circumvent the difficulties associated with excessive spatial localization or to consider size effects. Further work should focus on the construction of more advanced constitutive models within the proposed framework and their validation from experimental observations.

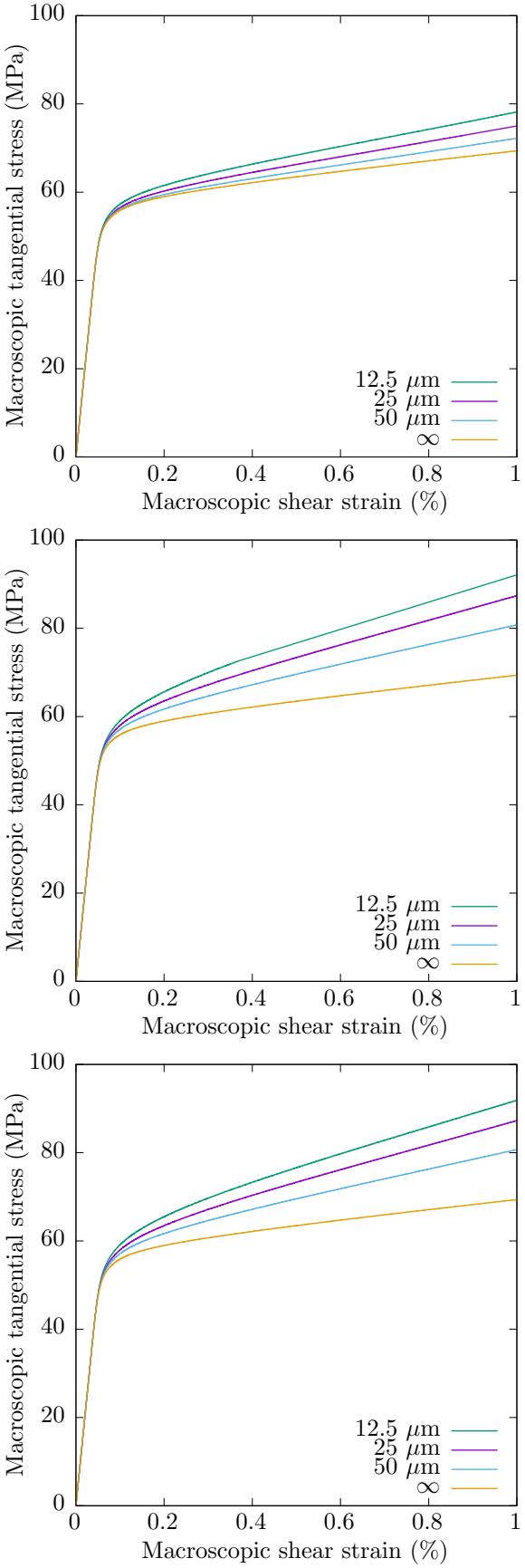

Fig. 5 Stress-strain diagrams obtained for a simple shear test for different grain sizes with the average-based (top), mixed (middle) and variance-based (bottom) non-local models.

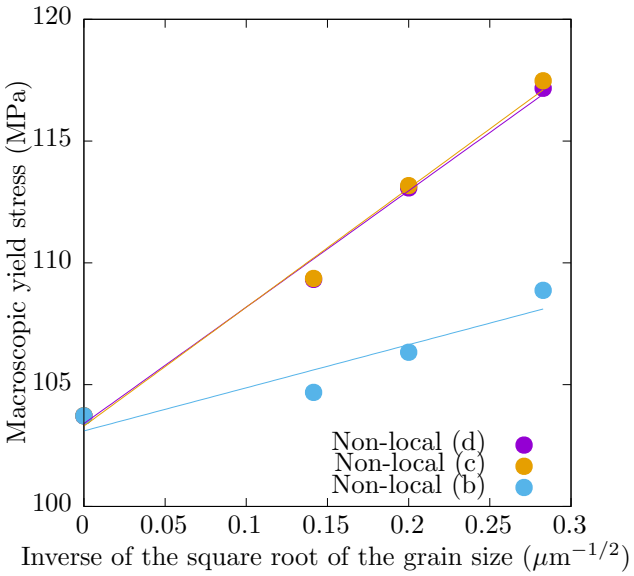

Fig. 6 Evolution of the yield stress as a function of the inverse of the square root of the average grain size. The yield stress is given by the von Mises equivalent stress corresponding to an equivalent plastic strain of 0.2%.

References

1. Aifantis, E.C., The physics of plastic deformation, Int. J. Plast. 3 (1987)
2. Ambati, M., Gerasimov, T., De Lorenzis, L., Phase-field modeling of ductile fracture, Comput Mech. 55 (2015)
3. Anand, L., Aslan, O., Chester, S.A., A large-deformation gradient theory for elasticplastic materials: Strain softening and regularization of shear bands, International Journal of Plasticity 30–31 (2012)
4. Andrade, F.X.C., César de Sá, J.M.A., Andrade Pires, F.M., A Ductile Damage Nonlocal Model of Integral-type at Finite Strains: Formulation and Numerical Issues, International Journal of Damage Mechanics 20 (2011)
5. Arsenlis, A., Parks, D., Crystallographic aspects of geometrically-necessary and statistically-stored dislocation density, Acta Mater. 47 (1999)
6. Bažant, Z.P., Lin, F.-B., Nonlocal yield-limit degradation, International Journal for Numerical Methods in Engineering 26 (1988)
7. Bažant, Z.P., Jirásek, M., Nonlocal Integral Formulations of Plasticity and Damage: Survey of Progress. Journal of Engineering Mechanics 128 (2002)
8. Benvenuti, E., Borino, G., Tralli, A., A thermodynamically consistent nonlocal formulation for damaging materials, European Journal of Mechanics A/Solids 21 (2003)
9. Berbenni, S., Taupin, V., Lebensohn, R.A., A fast Fourier transform-based mesoscale field dislocation mechanics study of grain size effects and reversible plasticity in polycrystals, J.Mech. Phys. Solids 135 (2020)
10. Borden, M.J., Hughes T.J.R., Landis, C.M., Verhoosel, C.V., A higher-order phase-field model for brittle fracture: formulation and analysis within the isogeometric analysis framework, Comput Methods Appl Mech Eng. 273 (2014)
11. Borino, G., Failla, B., Parrinello, F., A Symmetric Formulation for Nonlocal Damage Models, in: H. A. Mang, F. G. Rammerstorfer, J. Eberhardsteiner (Eds), Proceedings of the Fifth World Congress on Computational Mechanics (WCCM V), Vienna University of Technology, Vienna, Austria (2002)

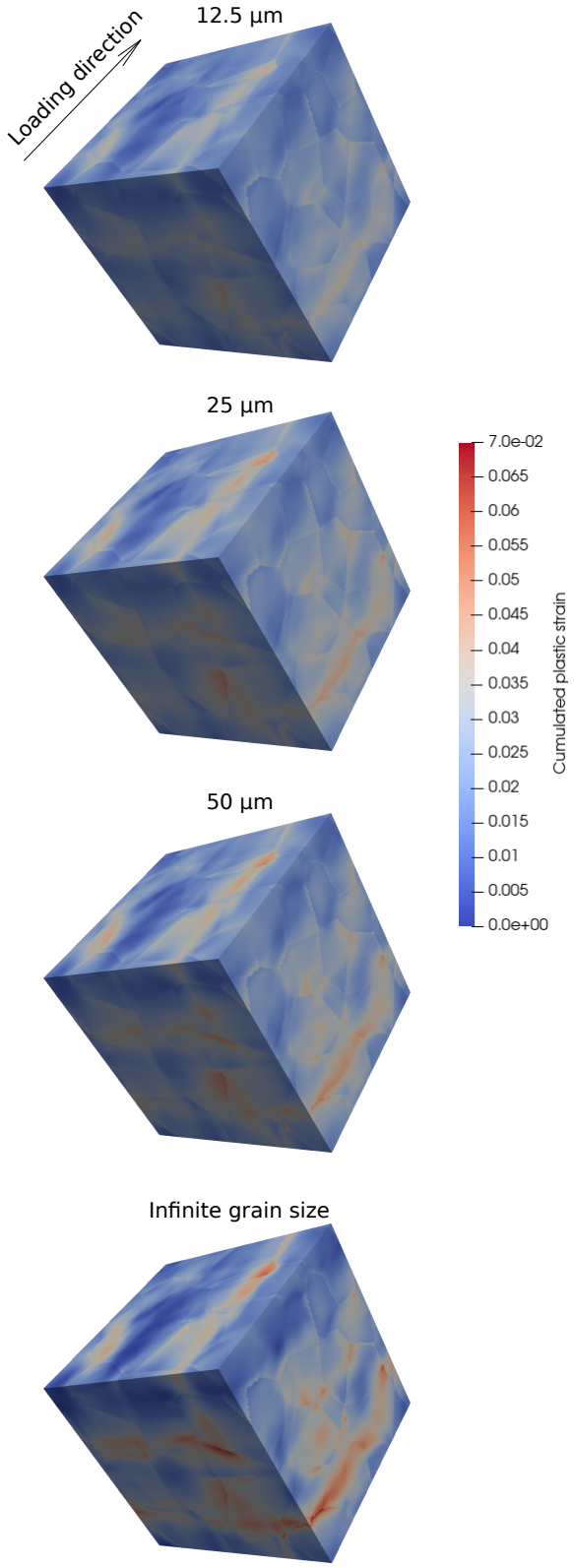

Fig. 7 Spatial distributions of the cumulated plastic strain obtained at the end of a simple shear test for different grain sizes with the variance-based non-local model.

12. Borino, G., Failla, B., Parrinello, F., A symmetric nonlocal damage theory. International Journal of Solids and Structures 40 (2003)
13. de Borst, R., Verhoosel, C.V., 2016, Gradient damage vs phase-field approaches for fracture: Similarities and differences, Computer Methods in Applied Mechanics and Engineering 312 (2016)
14. Cermelli, P., Gurtin. M.E., Geometrically necessary dislocations in viscoplastic single crystals and bicrystals undergoing small deformations, Int J Solids Struct 29 (2002)
15. Counts, W.A., Braginsky, M.V., Battaile, C.C., Holm, E.A., Predicting the HallPetch effect in fcc metals using non-local crystal plasticity, International Journal of Plasticity 24 (2008)
16. Desmorat, R., Gatuingt, F., Jirásek, M., Nonlocal models with damage-dependent interactions motivated by internal time, Engineering Fracture Mechanics 142 (2015)
17. Eisenlohr, P., Diehl, M., Lebensohn, R.A., Roters, F., A spectral method solution to crystal elasto-viscoplasticity at finite strains, International Journal of Plasticity 46 (2013)
18. Fleck, N.A., Muller, G.M., Ashby, M.F., Hutchinson, J.W., Strain gradient plasticity: Theory and experiment. Acta Metall. Mater. 42 (1994)
19. Fleck, N., Hutchinson, J., Strain gradient plasticity, Advances in Applied Mechanics 33, 296–361 (1997)
20. Fleck, N.A., Hutchinson, J.W., A reformulation of strain gradient plasticity, J. Mech. Phys. Solids 49 (2001)
21. Forest, S., Strain gradient crystal plasticity : thermomechanical formulations and applications, Journal of the Mechanical Behaviour of Materials 13 (2002)
22. Frémond, M., Nedjar, B., Damage, gradient of damage and principle of virtual power, Int J Solids Struct. 33 (1996)
23. Gao, H., Huang, Y., Taylor-based nonlocal theory of plasticity, Int. J. Solid Struct. 38 (2001)
24. Germain, P., Nguyen, Q.S., Suquet, P., Continuum Thermodynamics. J. Appl. Mech. 50 (1983)
25. Gmati, H., Mareau, C., Ammar, A., El Arem, S., A phasefield model for brittle fracture of anisotropic materials, International Journal for Numerical Methods in Engineering 121 (2020)
26. Gudmundson, P., A unified treatment of strain gradient plasticity, J. Mech. Phys. Solids 52 (2004)
27. Haouala, S., Lucarini, S., Llorca, J., Segurado, J., Simulation of the Hall-Petch effect in FCC polycrystals by means of strain gradient crystal plasticity and FFT homogenization, J. Mech. Phys. Solids 134 (2020)
28. Hernandez Padilla, C.A., Markert, B., A coupled phase-field model for ductile fracture in crystal plasticity, PAMM 14 (2014)
29. Jin, L., Ding, Z., Li, D., Du, X., Experimental and numerical investigations on the size effect of moderate high-strength reinforced concrete columns under small-eccentric compression, International Journal of Damage Mechanics 27 (2017)
30. Jirásek, M., Rolshoven S., Comparison of integral-type nonlocal plasticity models for strain-softening materials, International Journal of Engineering Science 41 (2003)
31. Leblond, J.B., Perrin, G., Devaux, J., Bifurcation effects in ductile metals with nonlocal damage, ASME Journal of Applied Mechanics 61 (1994)
32. Lemaitre, J., A course on damage mechanics, second ed, Springer-Verlag Berlin Heidelberg GmbH (1996)
33. Mandel, J., Plasticit classique et viscoplasticit, CISM-Udine, Springer, Wien New York (1972)
34. Miehe, C., Welschinger, F., Hofacker, M., Thermodynamically-consistent phase field models of fracture: variational principles and multi-field FE implementations, J Numer Methods Eng. 83 (2009)
35. Moulinec, H., Suquet, P., A numerical method for computing the overall response of nonlinear composites with complex microstructure, Computer Methods in Applied Mechanics and Engineering 157 (1998)
36. Nguyen, Q.S., Some remarks on standard gradient models and gradient plasticity, Mathematics and Mechanics of Solids 20 (2014)

37. Nguyen, V.D., Pardoen, T., Noels, L., A nonlocal approach of ductile failure incorporating void growth, internal necking, and shear dominated coalescence mechanisms, Journal of the Mechanics and Physics of Solids 137 (2020)
38. Niordson, C.F., Kysar, J.W., Computational strain gradient crystal plasticity, Journal of the Mechanics and Physics of Solids 62 (2014)
39. Nix, W.D., Mechanical properties of thin films, Metall. Trans. A 20A (1989)
40. Nye, J.F., Some geometrical relations in dislocated crystals, Acta Metall. 1 (1953)
41. Peng, X.L., Huang, G.Y., Modeling dislocation absorption by surfaces within the framework of strain gradient crystal plasticity, International Journal of Solids and Structures 72 (2015)
42. Pham, K., Amor, H., Marigo, J.J., Maurini, C., Gradient damage models and their use to approximate brittle fracture. Int J Damage Mech. 20 (2011)
43. Pijaudier–Cabot, G., Bažant, Z.P., Nonlocal damage theory, Journal of Engineering Mechanics ASCE 113 (1987)
44. Pijaudier-Cabot, G., Haidar, K., and Dubé, J.F., Nonlocal damage model with evolving internal length, Int. J. Numer. Anal. Meth. Geomech. 28 (2004)
45. Polizzotto, C., Borino, G., Fuschi, P., A thermodynamically consistent formulation of nonlocal and gradient plasticity, Mechanics Research Communications 25 (1998)
46. Šilhavý, M., The Mechanics and Thermodynamics of Continuous Media, Springer-Verlag Berlin Heidelberg GmbH (1997)
47. Strömberg, L., Ristinmaa, M., FE formulation of a nonlocal plasticity theory. Comput. Methods Appl. Mech. Eng. 136 (1996)
48. Vermeer, P.A., and Brinkgreve, R.B.J., A new effective non-local strain measure for softening plasticity. Localization and bifurcation theory for soils and rocks, R. Chambon, J. Desrues, and I. Vardoulakis, eds., Balkema, Rotterdam, The Netherlands, 89–100 (1994)
49. Voyiadjis, G.Z., Abu Al-Ruba, R.K., Palazotto, A.N., Thermodynamic framework for coupling of non-local viscoplasticity and non-local anisotropic viscodamage for dynamic localization problems using gradient theory, International Journal of Plasticity 20 (2004)
50. Walsh, P.F., Fracture of plain concrete, Indian Concr. J. 46 (1972)
51. Wu, J-Y., A unified phase-field theory for the mechanics of damage and quasi-brittle failure. Journal of the Mechanics and Physics of Solids 103 (2017)
52. Wulfinghoff, S., Böhlke, T., Equivalent plastic strain gradient enhancement of single crystal plasticity: theory and numerics, Proc. R. Soc. A 468 (2012)
53. Wulfinghoff, S., Bayerschen, E., Böhlke, T., A gradient plasticity grain boundary yield theory. International Journal of Plasticity 51 (2013)

A Averaging properties of non-local variables

The construction of constitutive relations uses some specific averaging properties of non-local variables. These properties are briefly demonstrated here. Specifically, for any local internal variable $\boldsymbol{\beta}$, the time derivative of the spatial average $\boldsymbol{\mu}_\beta$ is given by:

$$\dot{\boldsymbol{\mu}}_\beta[\boldsymbol{X}] = \frac{1}{W}\int_{\mathscr{V}_c} w[\boldsymbol{X}'-\boldsymbol{X}]\left(\dot{\boldsymbol{\beta}}[\boldsymbol{X}']-\dot{\boldsymbol{\beta}}[\boldsymbol{X}]\right)d\boldsymbol{X}' + \dot{\boldsymbol{\beta}}[\boldsymbol{X}] \tag{82}$$

For any tensor field $\boldsymbol{m}$, whose rank is that of $\boldsymbol{\beta}$, the above expression leads to:

$$\begin{aligned}\overline{\boldsymbol{m}\bullet\dot{\boldsymbol{\mu}}}_\beta =& \frac{1}{\mathscr{V}_c}\frac{1}{W}\int_{\mathscr{V}_c}\int_{\mathscr{V}_c} w[\boldsymbol{X}'-\boldsymbol{X}]\boldsymbol{m}[\boldsymbol{X}]\bullet\left(\dot{\boldsymbol{\beta}}[\boldsymbol{X}']-\dot{\boldsymbol{\beta}}[\boldsymbol{X}]\right)d\boldsymbol{X}'d\boldsymbol{X} \\ &+ \frac{1}{\mathscr{V}_c}\int_{\mathscr{V}_c}\boldsymbol{m}[\boldsymbol{X}]\bullet\dot{\boldsymbol{\beta}}[\boldsymbol{X}]d\boldsymbol{X}\end{aligned} \tag{83}$$

Since the weight function w is even, the above expression becomes:

$$\begin{aligned}\overline{\boldsymbol{m} \bullet \dot{\boldsymbol{\mu}}_\beta} =& \frac{1}{\mathscr{V}_c}\frac{1}{W}\int_{\mathscr{V}_c}\int_{\mathscr{V}_c} w[\boldsymbol{X}'-\boldsymbol{X}]\left(\boldsymbol{m}[\boldsymbol{X}']-\boldsymbol{m}[\boldsymbol{X}]\right)\bullet\dot{\boldsymbol{\beta}}[\boldsymbol{X}]d\boldsymbol{X}'d\boldsymbol{X} \\ &+\frac{1}{\mathscr{V}_c}\int_{\mathscr{V}_c}\boldsymbol{m}[\boldsymbol{X}]\bullet\dot{\boldsymbol{\beta}}[\boldsymbol{X}]d\boldsymbol{X} \end{aligned} \tag{84}$$

$$= \overline{\boldsymbol{\mu}_m \bullet \dot{\boldsymbol{\beta}}} \tag{85}$$

Also, the time derivative of the spatial variance $\boldsymbol{\xi}_\beta$ is:

$$\begin{aligned}\dot{\boldsymbol{\xi}}_\beta[\boldsymbol{X}] =& \frac{1}{W}\int_{\mathscr{V}_c} w[\boldsymbol{X}'-\boldsymbol{X}]\left(\boldsymbol{\mu}_\beta[\boldsymbol{X}]-\boldsymbol{\beta}[\boldsymbol{X}']\right)\otimes\left(\dot{\boldsymbol{\mu}}_\beta[\boldsymbol{X}]-\dot{\boldsymbol{\beta}}[\boldsymbol{X}']\right)d\boldsymbol{X}' \\ &+\frac{1}{W}\int_{\mathscr{V}_c} w[\boldsymbol{X}'-\boldsymbol{X}]\left(\dot{\boldsymbol{\mu}}_\beta[\boldsymbol{X}]-\dot{\boldsymbol{\beta}}[\boldsymbol{X}']\right)\otimes\left(\boldsymbol{\mu}_\beta[\boldsymbol{X}]-\boldsymbol{\beta}[\boldsymbol{X}']\right)d\boldsymbol{X}' \\ &-\frac{1}{W}\int_{\mathscr{V}_c} w[\boldsymbol{X}'-\boldsymbol{X}]\left(\boldsymbol{\mu}_\beta[\boldsymbol{X}]-\boldsymbol{\beta}[\boldsymbol{X}]\right)\otimes\left(\dot{\boldsymbol{\mu}}_\beta[\boldsymbol{X}]-\dot{\boldsymbol{\beta}}[\boldsymbol{X}]\right)d\boldsymbol{X}' \\ &-\frac{1}{W}\int_{\mathscr{V}_c} w[\boldsymbol{X}'-\boldsymbol{X}]\left(\dot{\boldsymbol{\mu}}_\beta[\boldsymbol{X}]-\dot{\boldsymbol{\beta}}[\boldsymbol{X}]\right)\otimes\left(\boldsymbol{\mu}_\beta[\boldsymbol{X}]-\boldsymbol{\beta}[\boldsymbol{X}]\right)d\boldsymbol{X}' \\ &+\left(\boldsymbol{\mu}_\beta[\boldsymbol{X}]-\boldsymbol{\beta}[\boldsymbol{X}]\right)\otimes\left(\dot{\boldsymbol{\mu}}_\beta[\boldsymbol{X}]-\dot{\boldsymbol{\beta}}[\boldsymbol{X}]\right)+\left(\dot{\boldsymbol{\mu}}_\beta[\boldsymbol{X}]-\dot{\boldsymbol{\beta}}[\boldsymbol{X}]\right)\otimes\left(\boldsymbol{\mu}_\beta[\boldsymbol{X}]-\boldsymbol{\beta}[\boldsymbol{X}]\right)\end{aligned} \tag{86}$$

For any symmetric tensor $\boldsymbol{z}$, whose rank is twice that of $\boldsymbol{\beta}$, one obtains that:

$$\begin{aligned}\overline{\boldsymbol{z}\blacksquare\dot{\boldsymbol{\xi}}_\beta} =& \frac{1}{\mathscr{V}_c}\frac{2}{W}\int_{\mathscr{V}_c}\int_{\mathscr{V}_c} w[\boldsymbol{X}'-\boldsymbol{X}]\boldsymbol{z}[\boldsymbol{X}]\blacksquare\left(\left(\boldsymbol{\mu}_\beta[\boldsymbol{X}]-\boldsymbol{\beta}[\boldsymbol{X}]\right)\otimes\dot{\boldsymbol{\beta}}[\boldsymbol{X}]\right)d\boldsymbol{X}'d\boldsymbol{X} \\ &-\frac{1}{\mathscr{V}_c}\frac{2}{W}\int_{\mathscr{V}_c}\int_{\mathscr{V}_c} w[\boldsymbol{X}'-\boldsymbol{X}]\boldsymbol{z}[\boldsymbol{X}]\blacksquare\left(\left(\boldsymbol{\mu}_\beta[\boldsymbol{X}]-\boldsymbol{\beta}[\boldsymbol{X}']\right)\otimes\dot{\boldsymbol{\beta}}[\boldsymbol{X}']\right)d\boldsymbol{X}'d\boldsymbol{X} \\ &-\frac{1}{\mathscr{V}_c}2\int_{\mathscr{V}_c}\boldsymbol{z}[\boldsymbol{X}]\blacksquare\left(\left(\boldsymbol{\mu}_\beta[\boldsymbol{X}]-\boldsymbol{\beta}[\boldsymbol{X}]\right)\otimes\dot{\boldsymbol{\beta}}[\boldsymbol{X}]\right)d\boldsymbol{X}\end{aligned} \tag{87}$$

The evenness of the weight function allows re-writing the above expression as follows:

$$\begin{aligned}\overline{\boldsymbol{z}\blacksquare\dot{\boldsymbol{\xi}}_\beta} =& \frac{1}{\mathscr{V}_c}\frac{2}{W}\int_{\mathscr{V}_c}\int_{\mathscr{V}_c} w[\boldsymbol{X}'-\boldsymbol{X}]\boldsymbol{z}[\boldsymbol{X}]\blacksquare\left(\left(\boldsymbol{\mu}_\beta[\boldsymbol{X}]-\boldsymbol{\beta}[\boldsymbol{X}]\right)\otimes\dot{\boldsymbol{\beta}}[\boldsymbol{X}]\right)d\boldsymbol{X}'d\boldsymbol{X} \\ &-\frac{1}{\mathscr{V}_c}\frac{2}{W}\int_{\mathscr{V}_c}\int_{\mathscr{V}_c} w[\boldsymbol{X}'-\boldsymbol{X}]\boldsymbol{z}[\boldsymbol{X}']\blacksquare\left(\left(\boldsymbol{\mu}_\beta[\boldsymbol{X}']-\boldsymbol{\beta}[\boldsymbol{X}]\right)\otimes\dot{\boldsymbol{\beta}}[\boldsymbol{X}]\right)d\boldsymbol{X}'d\boldsymbol{X} \\ &-2\frac{1}{\mathscr{V}_c}\int_{\mathscr{V}_c}\boldsymbol{z}[\boldsymbol{X}]\blacksquare\left(\left(\boldsymbol{\mu}_\beta[\boldsymbol{X}]-\boldsymbol{\beta}[\boldsymbol{X}]\right)\otimes\dot{\boldsymbol{\beta}}[\boldsymbol{X}]\right)d\boldsymbol{X}\end{aligned} \tag{88}$$

For the purpose of conciseness, it is convenient to introduce the tensor field $\boldsymbol{x}$ such that:

$$\boldsymbol{x}[\boldsymbol{X}] = \boldsymbol{z}[\boldsymbol{X}]\bullet\boldsymbol{\mu}_\beta[\boldsymbol{X}] \tag{89}$$

Using the above definition, expression (88) becomes:

$$\begin{aligned}\overline{\boldsymbol{z}\blacksquare\dot{\boldsymbol{\xi}}_\beta} =& \frac{2}{W}\int_{\mathscr{V}_c}\int_{\mathscr{V}_c} w[\boldsymbol{X}'-\boldsymbol{X}]\left(\left(\boldsymbol{z}[\boldsymbol{X}']-\boldsymbol{z}[\boldsymbol{X}]\right)\bullet\boldsymbol{\beta}[\boldsymbol{X}]\right)\bullet\dot{\boldsymbol{\beta}}[\boldsymbol{X}]d\boldsymbol{X}'d\boldsymbol{X} \\ &-\frac{2}{W}\int_{\mathscr{V}_c}\int_{\mathscr{V}_c} w[\boldsymbol{X}'-\boldsymbol{X}]\left(\boldsymbol{x}[\boldsymbol{X}']-\boldsymbol{x}[\boldsymbol{X}]\right)\bullet\dot{\boldsymbol{\beta}}[\boldsymbol{X}]d\boldsymbol{X}'d\boldsymbol{X} \\ &+2\int_{\mathscr{V}_c}\left(\boldsymbol{z}[\boldsymbol{X}]\bullet\boldsymbol{\beta}[\boldsymbol{X}]\right)\bullet\dot{\boldsymbol{\beta}}[\boldsymbol{X}]d\boldsymbol{X}-2\int_{\mathscr{V}_c}\boldsymbol{x}[\boldsymbol{X}]\bullet\dot{\boldsymbol{\beta}}[\boldsymbol{X}]d\boldsymbol{X}\end{aligned} \tag{90}$$

$$= \overline{2\left(\boldsymbol{\mu}_z\bullet\boldsymbol{\beta}-\boldsymbol{\mu}_x\right)\bullet\dot{\boldsymbol{\beta}}} \tag{91}$$

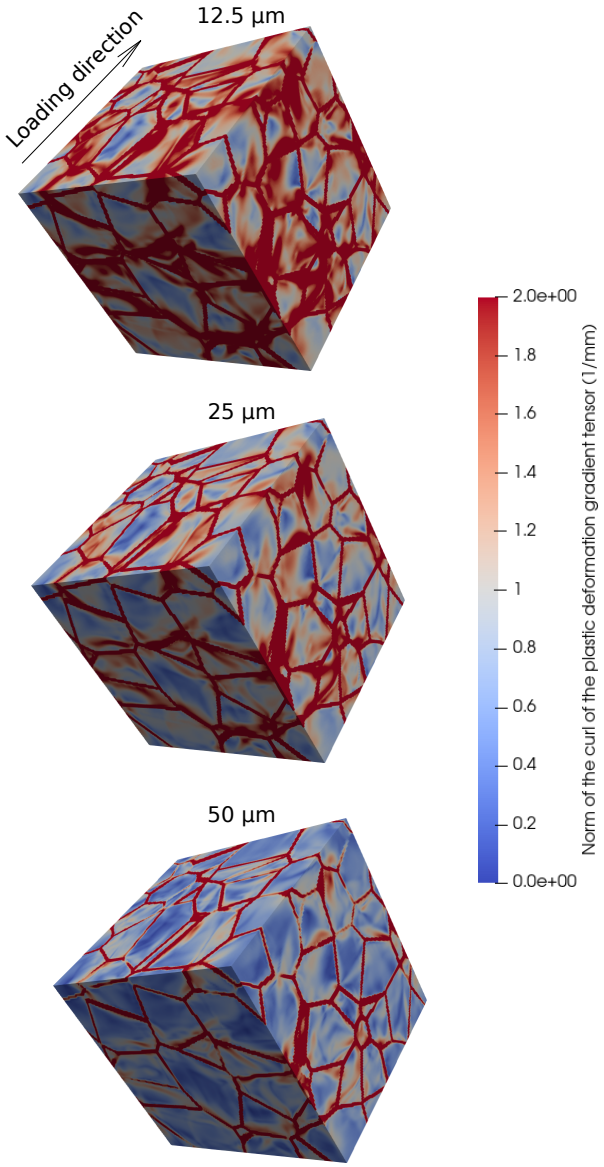

Fig. 8 Spatial distributions of $||\boldsymbol{\nabla} \times \boldsymbol{F}_p||$ obtained at the end of a simple shear test for different grain sizes with the variance-based non-local model.

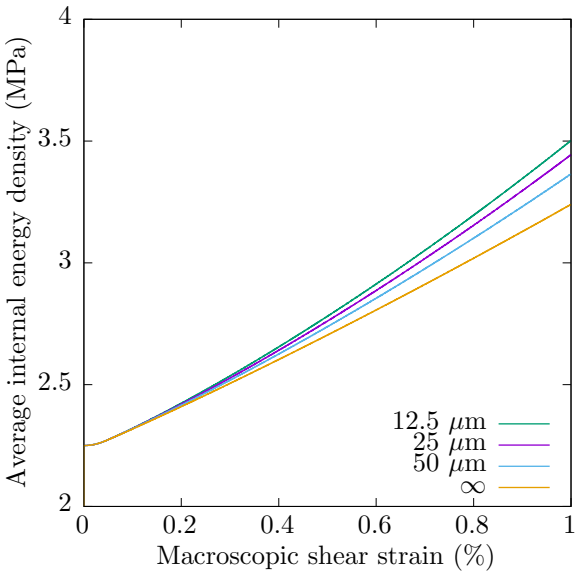

Fig. 9 Evolution of the average internal energy density calculated as a function of the macroscopic shear strain during a simple shear test for different grain sizes with the variance-based non-local model.